

Coggon, R.M., Teagle, D.A.H., Sylvan, J.B., Reece, J., Estes, E.R., Williams, T.J., Christeson, G.L., and the Expedition 390/393 Scientists

Proceedings of the International Ocean Discovery Program Volume 390/393 publications.iodp.org







Contents

- 1 Abstract
- 1 Introduction
- 2 Methods and materials
- 3 Results
- 6 Data availability
- **6** Acknowledgments
- **7** References

Kevwords

International Ocean Discovery Program, JOIDES Resolution, Expedition 393, South Atlantic Transect, Site U1583, Oligocene, Miocene, Pliocene, Pleistocene, Neogene

Supplementary material

References (RIS)

MS 390393-202

Received 13 October 2023 Accepted 9 January 2024 Published 5 April 2024

Data report: X-ray fluorescence scanning of sediment cores, IODP Expedition 390/393 Site U1583, South Atlantic Transect¹

Adriane R. Lam,² Chiara Amadori,² Chiara Borrelli,² Gail Christeson,² Emily Estes,² Laura Guertin,² Jennifer Hertzberg,³ Michael R. Kaplan,² Ravi Kiran Koorapati,⁴ Christopher M. Lowery,² Andrew McIntyre,² Julia S. Reece,² Claudio Robustelli Test,² Claire M. Routledge,² Patricia Standring,⁵ Jason B. Sylvan,² Mary Thompson,³ Alexandra Villa,² Yi Wang,² Shu Ying Wee,² Trevor Williams,² Jesse Yeon,³ Damon A.H. Teagle,² Rosalind M. Coggon,² and the Expedition 390/393 Scientists²

¹ Lam, A.R., Amadori, C., Borrelli, C., Christeson, G., Estes, E., Guertin, L., Hertzberg, J., Kaplan, M.R., Koorapati, R.K., Lowery, C.M., McIntyre, A., Reece, J.S., Robustelli Test, C., Routledge, C.M., Standring, P., Sylvan, J.B., Thompson, M., Villa, A., Wang, Y., Wee, S.Y., Williams, T., Yeon, J., Teagle, D.A.H., Coggon, R.M., and the Expedition 390/393 Scientists, 2024. Data report: X-ray fluorescence scanning of sediment cores, IODP Expedition 390/393 Site U1583, South Atlantic Transect. In Coggon, R.M., Teagle, D.A.H., Sylvan, J.B., Reece, J., Estes, E.R., Williams, T.J., Christeson, G.L., and the Expedition 390/393 Scientists, South Atlantic Transect. Proceedings of the International Ocean Discovery Program, 390/393: College Station, TX (International Ocean Discovery Program). https://doi.org/10.14379/iodp.proc.390393.202.2024

- ² Expedition 390/393 Scientists' affiliations. Correspondence author: alam@binghamton.edu
- ³Texas A&M University, United States.
- ⁴Binghamton University, United States.
- ⁵ University of Texas at Austin, United States.

Abstract

The western South Atlantic Ocean has not been drilled since the end of the Deep Sea Drilling Program, leading to a dearth of sedimentary sequences available from this sector of the Atlantic Ocean. In 2020–2022, a transect of new sites was drilled during International Ocean Discovery Program Expeditions 390C, 395E, 390, and 393 at 31°S and spanning from 28.8°W to 15.2°W. Here, we use X-ray fluorescence data, combined with shipboard magnetic susceptibility and natural gamma radiation, to characterize the sediments below the oligotrophic South Atlantic Gyre at Site U1583. These geochemical data add to the otherwise understudied southwest Atlantic Ocean.

1. Introduction

No scientific ocean drilling has occurred in the western South Atlantic since the termination of the Deep Sea Drilling Program (DSDP) in 1983. A new transect of sites was drilled close to DSDP Leg 3 sites in the western South Atlantic (Figure F1) during International Ocean Discovery Program (IODP) Expeditions 390C, 395E, 390, and 393, which took place between October 2020 and August 2022. These new sites provide the opportunity to address several research questions regarding how this region responded to past climatic and tectonic events through the Cenozoic. The South Atlantic Transect (SAT) sites, drilled around 31°S and spanning 26.4°W to 15.2°W, provide an excellent opportunity to study the oligotrophic portion of the South Atlantic Subtropical Gyre. Recovered sediments from this region can be used to reconstruct the paleoceanography of the region by investigating geologic global warming events (e.g., Yang et al., 2020), investigating the response of plankton communities to changes in gyre circulation and paleoclimate shifts (e.g., Lam et al., 2020), reconstructing the carbonate compensation depth at a relatively high spatial and temporal resolution (e.g., Dutkiewicz and Müller, 2021), and reconstructing bottom water masses in response to climate and ocean chemistry events through the Cenozoic (e.g., Gastaldello et al.,

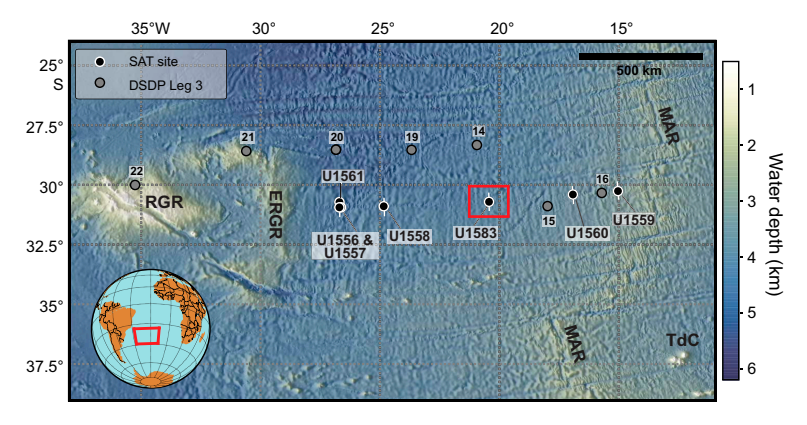


Figure F1. Bathymetric map of South Atlantic Ocean with location of sites drilled during Expeditions 390 and 393. DSDP Leg 3 sites are included for reference. Figure modified from Teagle et al. (2023). RGR = Rio Grande Rise, ERGR = eastern Rio Grande Rise, MAR = Mid-Atlantic Ridge, TdC = Tristan da Cunha hotspot.

2023). Moreover, such work will allow groundtruthing models of atmospheric and oceanic response to anthropogenic climate change.

The collection of sediment X-ray fluorescence (XRF) data is a fundamental tool to gain new insights into environmental changes because this qualitative geochemical technique allows the high-resolution acquisition of elemental information obtained in a nondestructive manner. XRF data can also be used to refine sedimentary units and define lithology (e.g., Penkrot et al., 2018; Taylor et al., 2022), infer the relative input of terrigenous versus biogenic material and wind strength through time, determine the relative oxygen availability at the seafloor, and so on (reviewed in Croudace and Rothwell, 2015). In this data report, we present an XRF data set for Site U1583 along its splice (see XRF in **Supplementary material**), a nearly complete record from the Oligocene to recent. We did not scan any basement lithologies for this data report.

Site U1583 is located in the central part of the transect atop 30.6 Ma oceanic crust located at 30°42.6175′S, 20°26.0336′W, at 4210 meters water depth. Nearby DSDP Sites 14 and 15 are situated to the north and east, respectively (Figure F1). Six holes were drilled at Site U1583. However, only two holes (U1583C and U1583E) recovered the majority of the sediments. Hole U1583C missed the mudline but recovered the sediment/basement interface, whereas Hole U1583E recovered the mudline but was terminated a few meters above basement (Teagle et al., 2024). Therefore, Holes U1583C and U1583E were used to create the splice for Site U1583. This site contains nannofossil ooze and foraminiferal ooze with varying amounts of clay in the lowermost cores (12H–3H) and alternating clay and nannofossil ooze with clay in the uppermost cores (3H–1H) (Teagle et al., 2023). Complementary XRF data sets have been developed for the other SAT sites, as follows: U1556 (Wang et al., 2024), U1557 (Lowery et al., 2024), U1558 (Villa et al., 2024), U1559 (Robustelli Test et al., 2024), U1560 (Amadori et al., 2024), and U1561 (Routledge et al., 2024).

2. Methods and materials

Core sections comprising the splice for Site U1583 were scanned on the fourth-generation Avaatech XRF Core Scanner (XRF 2) at the IODP Gulf Coast Repository in College Station, Texas (USA). The instrument is fitted with a water-cooled, 100 W rhodium side-window X-ray tube, a Brightspec SiriusSD silicon drift detector, and a Topaz-X high-resolution digital multichannel analyzer. Each archive section half was scanned at three excitation levels to measure different elements: 10 kV (with no filter) for major and minor elements (including Al, Si, K, Ca, Ti, Mn, Fe, Cr, P, S, and possibly Mg), 30 kV (with a thick Pd filter) for heavier major and minor elements and geologically relevant trace elements (including Ca, Ti, Mn, Fe, Ni, Sr, Rb, Zr, and Zn), and 50 kV (with a Cu filter) for heavier trace elements (including Sr, Rb, Zr, and Ba). The cross-core and downcore slits were set to 12 and 10 mm, respectively. Count times for the 10 and 30 kV scans

were set to 6 s, whereas count time was set to 10 s for the 50 kV scan. The current was set to 0.15, 1.24, and 0.75 mA for the 10, 30, and 50 kV scans, respectively.

2.1. Core preparation

Archive section halves were first equilibrated to room temperature. The surface of each section was gently scraped with a glass slide to expose a fresh surface and to level the core surface. The scraping was performed across the core (parallel to bedding planes) to ensure that no material was shifted stratigraphically. The glass slide was cleaned between each scrape to reduce any mixing of sediments. In the case of soupy intervals, several large Kimwipes were laid across the intervals to soak up excess water, and the intervals were flattened gently using a glass slide. Once the sediments were cleaned and flattened as much as possible, a 4 μ m thick Ultralene film was laid across the core and carefully taped to the edges of the core liner to prevent movement of the film. The film was put in place to prevent contamination of the XRF detector as it took measurements downsection.

2.2. Sample selection

The sections of Site U1583 that were included in the splice were scanned at a 5 cm resolution (0–9.613 and 24.385–140.023 m core composite depth below seafloor [CCSF]). Select sections (9.613–24.301 m CCSF) from Hole U1583C were scanned at a 2 cm resolution to capture major paleoclimatic intervals (e.g., the Miocene Climate Optimum) at a higher resolution. Sample locations were double-checked prior to scanning, and they were manually adjusted to avoid measurements over gaps, cracks, fractures, and so on.

2.3. Quality control

To ensure consistent data quality from the XRF core scanner, standards were run at all three excitation levels at the beginning and end of each scanning day. At the beginning of each scanning day, 20 replicates were run at each excitation level to warm up the instrument; at the end of the day, no replicates were run.

Raw spectral peaks were processed into peak areas and exported as count data for different elements using the Brightspec XRF spectral processing software bAxil. Quality control of the data was based on two criteria. Samples with throughput values of <150,000 counts/s on the 10 kV scan were removed because these values may indicate the prism did not fully land on the sample surface or the prism landed on a void. Samples with a positive argon (Ar) value were also removed because positive Ar values indicate the detector was measuring ambient air that may have resulted from the prism not landing flush with the sample surface or landing on a void in the sample surface. Quality control based on throughput and Ar values was carried out using an R code (R Core Team, 2023; available at https://github.com/Ravikiran2316/IODP-Exp.-390-393-XRF).

3. Results

3.1. Correlation between elements

We created crossplots using raw element counts of elements that are paleoceanographically and environmentally important to preliminarily determine the relationship between elements. For example, there is a strong correlation between titanium (Ti) and iron (Fe), indicating that both are sourced from terrestrial settings (Figure F2B). A strong correlation between these two elements also indicates that iron is likely unaffected by diagenetic remobilization at Site U1583, as good correlation between iron and titanium indicates very little diagenetic influence (Rothwell and Croudace, 2015). In addition, we conducted a Spearman's rank correlation to determine which elements correlate with one another (Figure F3). Elements that are generally indicative of productivity, such as silicon (Si), barium (Ba), and strontium (Sr), mostly have a negative correlation with calcium (Ca). In contrast, Si and Ba are positively correlated with elements that are typically indicative of terrigenous indicators, such as iron (Fe), zirconium (Zr), titanium (Ti), potassium (K), and aluminum (Al). Strontium has a negative correlation with most elements, except for nickel (Ni),

sulfur (S), and bromine (Br), but these positive correlations are generally weaker (with ρ values ranging from 0.11 to 0.34; a ρ value of ± 1 indicates a strong negative or positive correlation).

The most strongly positively correlated values ($\rho > 0.85$) include Mn and Fe, Zr and Ti, Ti and K, Ti and Al, Ti and Si, K and Al, K and Si, and Al and Si. The most weakly positively correlated values ($\rho < 0.15$) include Sr and Ni, Sr and Br, Ba and Br, Mn and Br, Zr and S, and Ti and S. The most weakly negatively correlated values ($\rho < -0.15$) include Ba and Ca, Ca and Ni, Sr and Zr, Ba and S, and Fe and S.

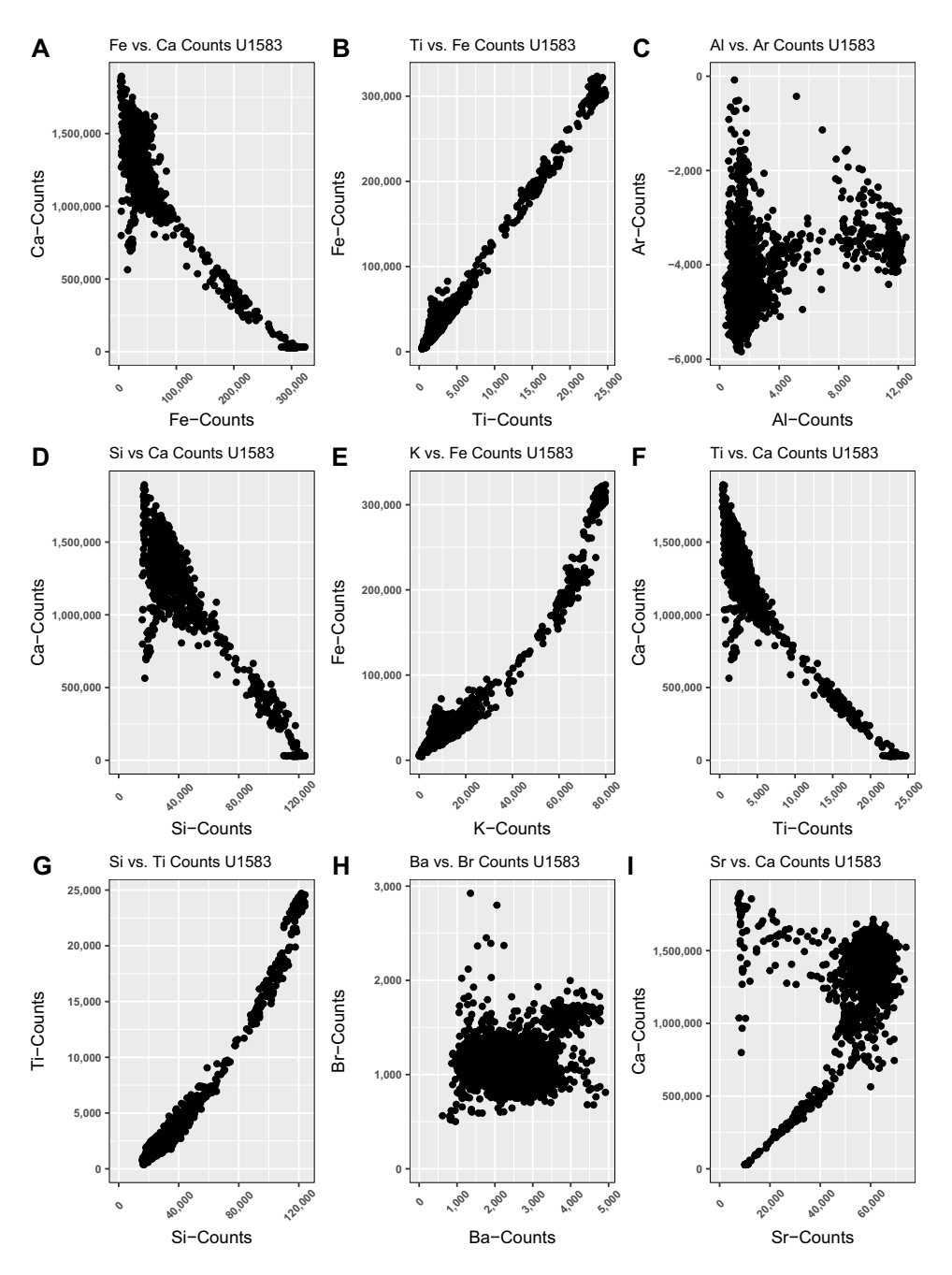


Figure F2. Crossplots of selected element raw counts of common paleoceanographically important elements from XRF scanning, Site U1583. A. Fe versus Ca. B. Ti versus Fe. C. Al versus Ar. D. Si versus Ca. E. K versus Fe. F. Ti versus Ca. G. Si versus Ti. H. Ba versus Br. I. Sr versus Ca. See Figure F3 for Spearman's rank correlation.

3.2. Stratigraphic trends

Select elemental counts (Ca, Fe, Ti, Al, Si, K, and Zr) were plotted stratigraphically with shipboard magnetic susceptibility (MS) and natural gamma radiation (NGR; splitting out U, Th, and K) (Coggon et al., 2024) and sedimentary units (Teagle et al., 2024) to determine the relationship between XRF count data and shipboard measurements (Figure F4). Major geologic epochs are inferred from shipboard age models based on calcareous microfossil biostratigraphy and interpreted geomagnetic reversal boundaries (Teagle et al., 2024). In general, the XRF counts, MS, and NGR data are synchronous from the Oligocene to the Pliocene/Pleistocene because the trends largely move and change with one another through the study interval. Throughout the Oligocene, counts generally remain stable for all elements, with some variability evident around 110 m CCSF, especially for Ca.

Both MS and NGR increase upcore at the Oligocene/Miocene boundary. Into the Miocene, MS, NGR, and count data are stable to around 35 m CCSF. From \sim 35 to \sim 20 m CCSF, within the Miocene to early Pliocene–Pleistocene interval, MS and NGR begin to increase in a stepwise fashion, with three major steps evident (Figure F4). The three steps are also evident in the XRF count data: Ca counts decline, whereas Fe, Ti, Al, Si, K, and Zr counts increase. The last major step in the data sets occurs right after the Miocene/Pliocene boundary.

Within the Pliocene–Pleistocene interval around 20 m CCSF, all proxies exhibit a sharp decrease upcore, except Ca, which exhibits a sharp increase. XRF count data within the Pliocene–Pleistocene interval are higher than those recorded from the Oligocene interval (Ca counts are lower than the Oligocene interval). MS, NGR, and XRF counts exhibit more variability within the Pliocene–Pleistocene interval compared to the Oligocene to ~Middle Miocene intervals.

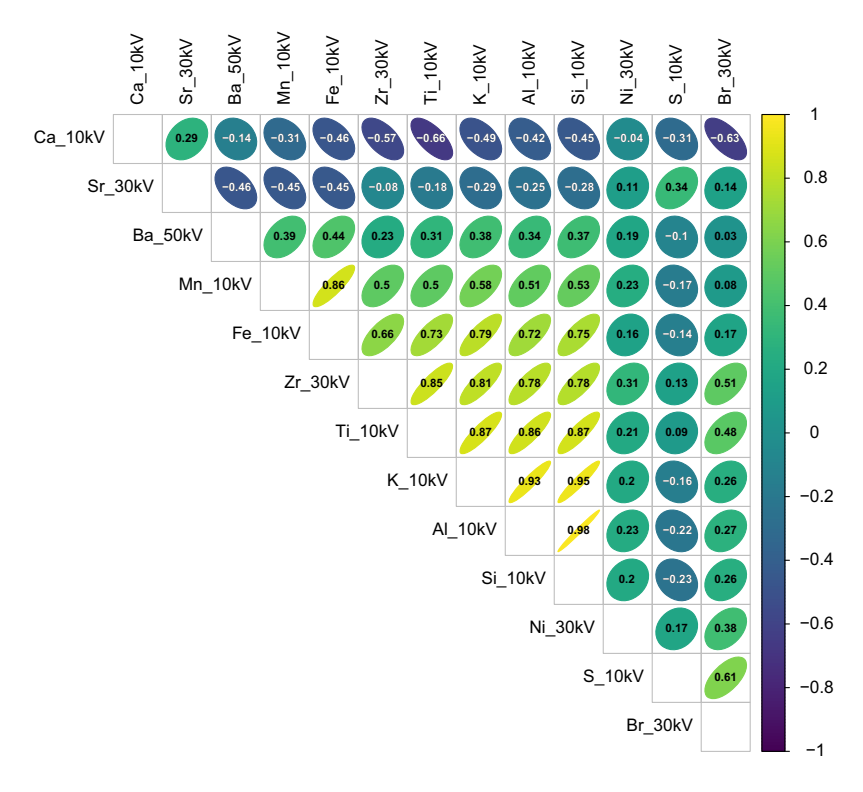


Figure F3. Correlogram for elements above XRF detection limits (>1000 counts/s), Site U1583 splice. Spearman's rank correlation was used to determine the correlation between elements. Green to yellow colors indicate a positive correlation (black ρ values), and teal to purple colors indicate a negative correlation (white ρ values). The more spherical the shapes are within the correlogram, the less correlated the elements are, whereas greater ellipticity of the shapes is indicative of a higher correlation. The ρ values for each correlation are plotted in the center of each correlated element pair. The following elements were used from the 10 kV excitation energy: Al, Si, S, K, Ca, Ti, Mn, and Fe; from the 30 kV excitation energy: Ni, Br, Sr, Zr; and from the 50 kV excitation energy: Ba.

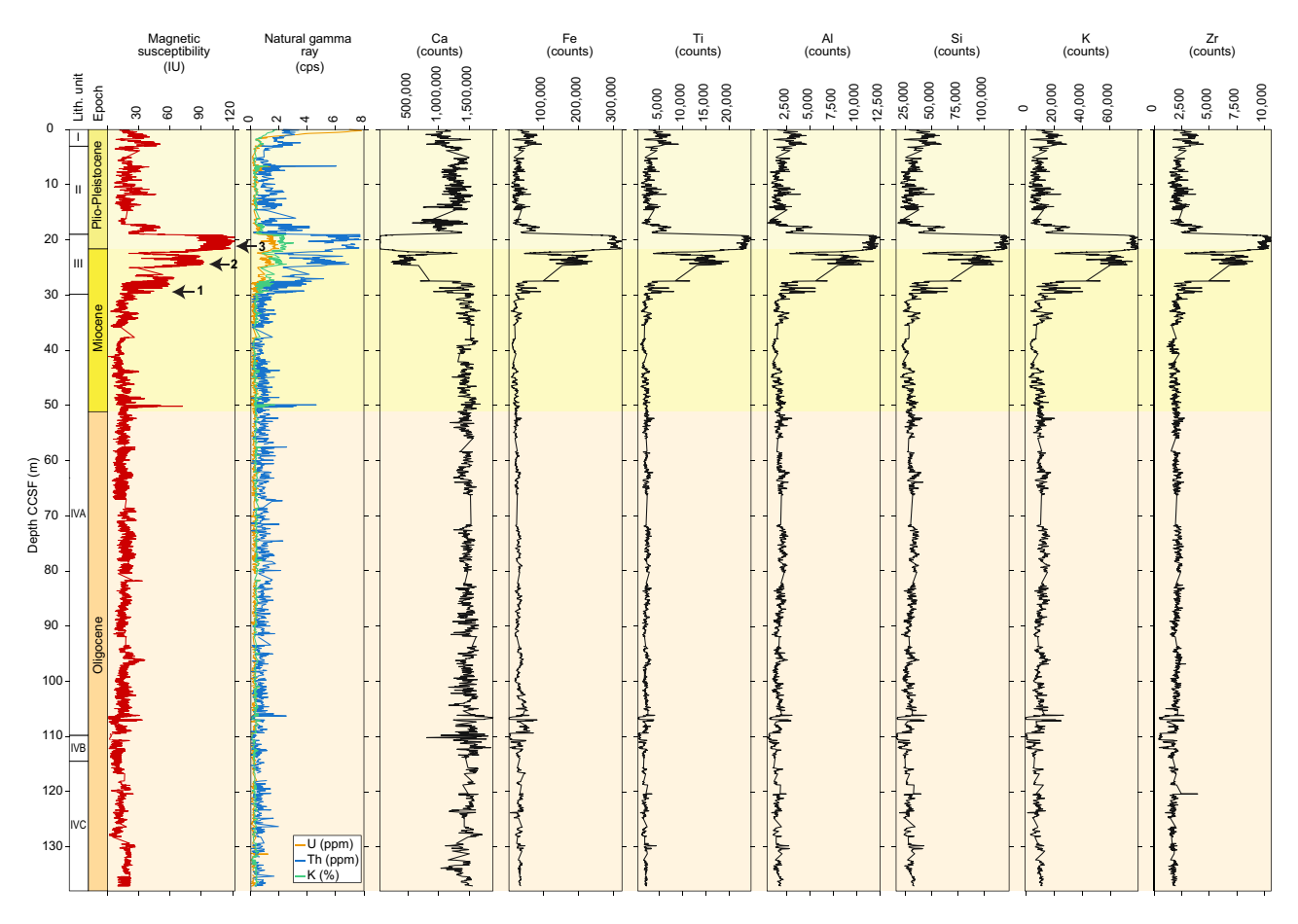


Figure F4. MS, spectral gamma ray, and scanning XRF counts of selected elements, Site U1583. MS uses whole-round measurements. The three arrows on the MS curve denote the three steps observed in all data sets. NGR data are shown for concentrations of the individual radioactive elements: U (parts per million), Th (parts per million), and K (weight percent). See Figure F3 for the excitation energies for each element.

4. Data availability

XRF data at all three excitation levels are included here as supplementary material (see XRF in **Supplementary material**) and permanently archived at PANGAEA (https://Pangea.de).

5. Acknowledgments

We are grateful to the crew, staff, and technicians on the R/V *JOIDES Resolution* for Expeditions 390C, 395E, 390, and 393, as well as the technicians and staff at the Gulf Coast Repository, particularly Michelle Penkrot. XRF scans reported here comprise the programmatic scanning for Expeditions 390C, 395E, 390, and 393 and were funded by the National Science Foundation (NSF) in agreement with the US Science Support Program (USSSP). We also acknowledge XRF scanning travel support for US scientists administered by USSSP and support of E.R. Estes and T.J. Williams through NSF award OCE 1326927. The authors wish to thank Matthew Jones for comments and edits that strengthened this data report.

References

- Amadori, C., Borrelli, C., Christeson, G., Estes, E., Guertin, L., Hertzberg, J., Kaplan, M.R., Koorapati, R.K., Lam, A.R., Lowery, C.M., McIntyre, A., Reece, J., Robustelli Test, C., Routledge, C.M., Standring, P., Sylvan, J.B., Thompson, M., Villa, A., Wang, Y., Wee, S.Y., Williams, T., Yeon, J., Teagle, D.A.H., Coggon, R.M., and the Expedition 390/393 Scientists, 2024. Data report: X-ray fluorescence scanning of sediment cores, IODP Expedition 390/393 Site U1560, South Atlantic Transect. In Coggon, R.M., Teagle, D.A.H., Sylvan, J.B., Reece, J., Estes, E.R., Williams, T.J., Christeson, G.L., and the Expedition 390/393 Scientists, South Atlantic Transect. Proceedings of the International Ocean Discovery Program, 390/393: College Station, TX (International Ocean Discovery Program). https://doi.org/10.14379/iodp.proc.390393.205.2024
- Coggon, R.M., Teagle, D.A.H., Sylvan, J.B., Reece, J., Estes, E.R., Williams, T.J., Christeson, G.L., Aizawa, M., Albers, E., Amadori, C., Belgrano, T.M., Borrelli, C., Bridges, J.D., Carter, E.J., D'Angelo, T., Dinarès-Turell, J., Doi, N., Estep, J.D., Evans, A., Gilhooly, W.P., III, Grant, L.C.J., Guérin, G.M., Harris, M., Hojnacki, V.M., Hong, G., Jin, X., Jonnalagadda, M., Kaplan, M.R., Kempton, P.D., Kuwano, D., Labonte, J.M., Lam, A.R., Latas, M., Lowery, C.M., Lu, W., McIntyre, A., Moal-Darrigade, P., Pekar, S.F., Robustelli Test, C., Routledge, C.M., Ryan, J.G., Santiago Ramos, D., Shchepetkina, A., Slagle, A.L., Takada, M., Tamborrino, L., Villa, A., Wang, Y., Wee, S.Y., Widlansky, S.J., Yang, K., Kurz, W., Prakasam, M., Tian, L., Yu, T., and Zhang, G., 2024. Expedition 390/393 methods. In Coggon, R.M., Teagle, D.A.H., Sylvan, J.B., Reece, J., Estes, E.R., Williams, T.J., Christeson, G.L., and the Expedition 390/393 Scientists, South Atlantic Transect. Proceedings of the International Ocean Discovery Program, 390/393.102.2024
- Croudace, I.W., and Rothwell, R.G. (Eds.), 2015. Micro-XRF Studies of Sediment Cores: Applications of a non-destructive tool for the environmental sciences: (Springer Dordrecht). https://doi.org/10.1007/978-94-017-9849-5
- Dutkiewicz, A., and Müller, R.D., 2021. The carbonate compensation depth in the South Atlantic Ocean since the Late Cretaceous. Geology, 49(7):873–878. https://doi.org/10.1130/G48404.1
- Gastaldello, M.E., Agnini, C., Westerhold, T., Drury, A.J., Sutherland, R., Drake, M.K., Lam, A.R., Dickens, G.R., Dallanave, E., Burns, S., and Alegret, L., 2023. The Late Miocene-Early Pliocene biogenic bloom: an integrated study in the Tasman Sea. Paleoceanography and Paleoclimatology, 38(4):e2022PA004565. https://doi.org/10.1029/2022PA004565
- Lam, A.R., Amadori, C., Borrelli, C., Christeson, G., Estes, E., Guertin, L., Hertzberg, J., Kaplan, M.R., Koorapati, R.K., Lowery, C.M., McIntyre, A., Reece, J.S., Robustelli Test, C., Routledge, C.M., Standring, P., Sylvan, J.B., Thompson, M., Villa, A., Wang, Y., Wee, S.Y., Williams, T., Yeon, J., Teagle, D.A.H., Coggon, R.M., and the Expedition 390/393 Scientists, 2024. Supplementary material, https://doi.org/10.14379/iodp.proc.390393.202supp.2024. In Lam, A.R., Amadori, C., Borrelli, C., Christeson, G., Estes, E., Guertin, L., Hertzberg, J., Kaplan, M.R., Koorapati, R.K., Lowery, C.M., McIntyre, A., Reece, J.S., Robustelli Test, C., Routledge, C.M., Standring, P., Sylvan, J.B., Thompson, M., Villa, A., Wang, Y., Wee, S.Y., Williams, T., Yeon, J., Teagle, D.A.H., Coggon, R.M., and the Expedition 390/393 Scientists, 2024. Data report: X-ray fluorescence scanning of sediment cores, IODP Expedition 390/393 Site U1583, South Atlantic Transect. In Coggon, R.M., Teagle, D.A.H., Sylvan, J.B., Reece, J., Estes, E.R., Williams, T.J., Christeson, G.L., and the Expedition 390/393 Scientists, South Atlantic Transect. Proceedings of the International Ocean Discovery Program, 390/393: College Station, TX (International Ocean Discovery Program).
- Lam, A.R., Leckie, R.M., and Patterson, M.O., 2020. Illuminating the past to see the future of western boundary currents: micropaleontological investigations of the Kuroshio Current extension. Oceanography, 33(2):65–67. https://doi.org/10.5670/oceanog.2020.219
- Lowery, C.M., Amadori, C., Borrelli, C., Christeson, G., Estes, E., Guertin, L., Hertzberg, J., Kaplan, M.R., Koorapati, R.K., Lam, A.R., McIntyre, A., Reece, J., Robustelli Test, C., Routledge, C.M., Standring, P., Sylvan, J.B., Thompson, M., Villa, A., Wang, Y., Wee, S.Y., Williams, T., Yeon, J., Teagle, D.A.H., Coggon, R.M., and the Expedition 390/393 Scientists, 2024. Data report: X-ray fluorescence scanning of sediment cores, Site U1557, South Atlantic Transect. In Coggon, R.M., Teagle, D.A.H., Sylvan, J.B., Reece, J., Estes, E.R., Williams, T.J., Christeson, G.L., and the Expedition 390/393 Scientists, South Atlantic Transect. Proceedings of the International Ocean Discovery Program, 390/393: College Station, TX (International Ocean Discovery Program).
 https://doi.org/10.14379/iodp.proc.390393.201.2024
- Penkrot, M.L., Jaeger, J.M., Cowan, E.A., St-Onge, G., and LeVay, L., 2018. Multivariate modeling of glacimarine lithostratigraphy combining scanning XRF, multisensory core properties, and CT imagery: IODP Site U1419. Geosphere, 14(4):1935–1960. https://doi.org/10.1130/GES01635.1
- R Core Team, 2023. R: A language and environment for statistical computing. R Foundation for Statistical Computing. https://www.r-project.org/
- Robustelli Test, C., Amadori, C., Borrelli, C., Christeson, G., Estes, E., Guertin, L., Hertzberg, J., Kaplan, M.R., Koorapati, R.K., Lam, A.R., Lowery, C.M., McIntyre, A., Reece, J., Routledge, C.M., Standring, P., Sylvan, J.B., Thompson, M., Villa, A., Wang, Y., Wee, S.Y., Williams, T., Yeon, J., Teagle, D.A.H., Coggon, R.M., and the Expedition 390/393 Scientists, 2024. Data report: X-ray fluorescence scanning of sediment cores, IODP Expedition 390/393 Site U1559, South Atlantic Transect. In Coggon, R.M., Teagle, D.A.H., Sylvan, J.B., Reece, J., Estes, E.R., Williams, T.J., Christeson, G.L., and the Expedition 390/393 Scientists, South Atlantic Transect. Proceedings of the International Ocean Discovery Program, 390/393: College Station, TX (International Ocean Discovery Program). https://doi.org/10.14379/iodp.proc.390393.204.2024
- Rothwell, R.G., and Croudace, I.w., 2015. Twenty years of XRF core scanning marine sediments: what do geochemical proxies tell us? In Croudace, I.W., and Rothwell, R.G. (Eds.), Micro-XRF Studies of Sediment Cores: Applications of a non-destructive tool for the environmental sciences. Dordrecht (Springer Netherlands), 25–102. https://doi.org/10.1007/978-94-017-9849-5_2

- Routledge, C.M., Amadori, C., Borrelli, C., Christeson, G., Estes, E., Guertin, L., Hertzberg, J., Kaplan, M.R., Koorapati, R.K., Lam, A.R., Lowery, C.M., McIntyre, A., Reece, J., Robustelli Test, C., Standring, P., Sylvan, J.B., Thompson, M., Villa, A., Wang, Y., Wee, S.Y., Williams, T., Yeon, J., Teagle, D.A.H., Coggon, R.M., and the Expedition 390/393 Scientists, 2024. Data report: X-ray fluorescence scanning of sediment cores, IODP Expedition 390/393 Site U1561, South Atlantic Transect. In Coggon, R.M., Teagle, D.A.H., Sylvan, J.B., Reece, J., Estes, E.R., Williams, T.J., Christeson, G.L., and the Expedition 390/393 Scientists, South Atlantic Transect. Proceedings of the International Ocean Discovery Program, 390/393: College Station, TX (International Ocean Discovery Program). https://doi.org/10.14379/iodp.proc.390393.207.2024
- Taylor, S.P., Patterson, M.O., Lam, A.R., Jones, H., Woodard, S.C., Habicht, M.H., Thomas, E.K., and Grant, G.R., 2022. Expanded North Pacific subtropical gyre and heterodyne expression during the Mid-Pleistocene. Paleoceanography and Paleoclimatology, 37(5):e2021PA004395. https://doi.org/10.1029/2021PA004395
- Teagle, D.A.H., Reece, J., Coggon, R.M., Sylvan, J.B., Christeson, G.L., Williams, T.J., Estes, E.R., and the Expedition 393 Scientists, 2023. Expedition 393 Preliminary Report: South Atlantic Transect 2. International Ocean Discovery Program. https://doi.org/10.14379/iodp.pr.393.2023
- Teagle, D.A.H., Reece, J., Williams, T.J., Coggon, R.M., Sylvan, J.B., Estes, E.R., Christeson, G.L., Albers, E., Amadori, C., Belgrano, T.M., D'Angelo, T., Doi, N., Evans, A., Guérin, G.M., Harris, M., Hojnacki, V.M., Hong, G., Jin, X., Jonnalagadda, M., Kuwano, D., Labonte, J.M., Lam, A.R., Latas, M., Lu, W., Moal-Darrigade, P., Pekar, S.F., Robustelli Test, C., Ryan, J.G., Santiago Ramos, D., Shchepetkina, A., Villa, A., Wee, S.Y., Widlansky, S.J., Aizawa, M., Borrelli, C., Bridges, J.D., Carter, E.J., Dinarès-Turell, J., Estep, J.D., Gilhooly, W.P., III, Grant, L.C.J., Kaplan, M.R., Kempton, P.D., Lowery, C.M., McIntyre, A., Routledge, C.M., Slagle, A.L., Takada, M., Tamborrino, L., Wang, Y., Yang, K., Kurz, W., Prakasam, M., Tian, L., Yu, T., and Zhang, G., 2024. Site U1583. In Coggon, R.M., Teagle, D.A.H., Sylvan, J.B., Reece, J., Estes, E.R., Williams, T.J., Christeson, G.L., and the Expedition 390/393 Scientists, South Atlantic Transect. Proceedings of the International Ocean Discovery Program, 390/393: College Station, TX (International Ocean Discovery Program). https://doi.org/10.14379/iodp.proc.390393.107.2024
- Villa, A., Amadori, C., Borrelli, C., Christeson, G., Estes, E., Guertin, L., Hertzberg, J., Kaplan, M.R., Koorapati, R.K., Lam, A.R., Lowery, C.M., McIntyre, A., Reece, J., Robustelli Test, C., Routledge, C.M., Standring, P., Sylvan, J.B., Thompson, M., Wang, Y., Wee, S.Y., Williams, T., Yeon, J., Teagle, D.A.H., Coggon, R.M., and the Expedition 390/393 Scientists, 2024. Data report: X-ray fluorescence scanning of sediment cores, IODP Expedition 390/393 Site U1558, South Atlantic Transect. In Coggon, R.M., Teagle, D.A.H., Sylvan, J.B., Reece, J., Estes, E.R., Williams, T.J., Christeson, G.L., and the Expedition 390/393 Scientists, South Atlantic Transect. Proceedings of the International Ocean Discovery Program, 390/393: College Station, TX (International Ocean Discovery Program). https://doi.org/10.14379/iodp.proc.390393.203.2024
- Wang, Y., Amadori, C., Borrelli, C., Christeson, G., Estes, E., Guertin, L., Hertzberg, J., Kaplan, M.R., Koorapati, R.K., Lam, A.R., Lowery, C.M., McIntyre, A., Reece, J., Robustelli Test, C., Routledge, C.M., Standring, P., Sylvan, J.B., Thompson, M., Villa, A., Wee, S.Y., Williams, T., Yeon, J., and the Expedition 390/393 Scientists, 2024. Data report: X-ray fluorescence scanning of sediment cores, IODP Expedition 390/393 Site U1556, South Atlantic Transect. In Coggon, R.M., Teagle, D.A.H., Sylvan, J.B., Reece, J., Estes, E.R., Williams, T.J., Christeson, G.L., and the Expedition 390/393 Scientists, South Atlantic Transect. Proceedings of the International Ocean Discovery Program, 390/393: College Station, TX (International Ocean Discovery Program). https://doi.org/10.14379/iodp.proc.390393.206.2024
- Yang, H., Lohmann, G., Krebs-Kanzow, U., Ionita, M., Shi, X., Sidorenko, D., Gong, X., Chen, X., and Gowan, E.J., 2020. Poleward shift of the major ocean gyres detected in a warming climate. Geophysical Research Letters, 47(5):e2019GL085868. https://doi.org/10.1029/2019GL085868